

# Anomalous surface currents in the tropical Indian Ocean

*Semyon A. Grodsky*<sup>1</sup>, *James A. Carton*<sup>1</sup>, and *Raghu Murtugudde*<sup>2</sup>

Submitted to the Geophysical Research Letters.

June 28, 2001

Revised

August 26, 2001

Accepted September 14, 2001

1. Department of Meteorology,

University of Maryland,

College Park, MD 20742

[senya@atmos.umd.edu](mailto:senya@atmos.umd.edu)

2. ESSIC

University of Maryland,

College Park, MD 20742

[ragu@essic.umd.edu](mailto:ragu@essic.umd.edu)

## Abstract

An anomalous climate event occurred in 1997 in the Indian Ocean with severe consequences for the surrounding continental areas. In response to an intensification of the trade winds, a westward gradient of SST and an anomalous reversal of the eastward surface currents with peak velocity anomalies exceeding 1 m/s were evident in the boreal autumn. A similar but weaker event took place in 1994. In this study we examine the observational record during the 1990s including surface drifter velocities, SST and altimeter sea level to confirm these dramatic changes. We examine the key momentum balance between wind-induced momentum flux and the pressure gradient force as well as the important role of horizontal temperature advection in the mixed layer heat response.

## 1. Introduction

In boreal autumn of 1997 the meteorological conditions in the tropical Indian Ocean were quite unusual. The trade winds extended equatorward and intensified by  $0.3 \text{ dyn/cm}^2$ . The zonal component of wind stress on the equator (normally eastward and weak this time of the year) reversed direction and increased by  $0.1 - 0.2 \text{ dyn/cm}^2$  as well. In response the eastern basin SST cooled by  $1^\circ\text{C}$  to  $3^\circ\text{C}$  along and south of the equator with a corresponding drop in sea level, while in the western basin there was substantial warming of SST albeit with a phase lag [Yu and Reinecker, 1999; Potemra and Lukas, 1999; Saji *et al.*, 1999; Webster *et al.*, 1999; Murtugudde *et al.*, 2000; Susanto *et al.*, 2001]. Recent modeling studies suggest the importance of horizontal advection within the mixed layer acting directly on the zonal gradient of mixed layer temperature in inducing a dipole SST pattern, and indirectly in forcing an east-west gradient in thermocline depth by redistributing mass [Murtugudde *et al.*, 2000]. Here we exploit the availability of direct observations of near-surface velocity to document these remarkable changes in the context of a 9-year record and examine the role of advection in thermodynamics along the equator.

Much of our empirical knowledge of the seasonal changes in the Indian Ocean surface currents comes from analyses of historical shipdrift observations [Cutler and Swallow, 1984; Rao *et al.*, 1989] and near surface drifter tracks [Molinari *et al.*, 1990]. The annual mean surface currents on the equator are eastward. Their seasonal variation has a well-pronounced semi-annual harmonic. During the boreal winter (JFM), the currents are dominated by the westward North Equatorial Current with speeds of 50 cm/s extending from  $90^\circ \text{ E}$  to Africa. During spring (AMJ) and late autumn (OND), the eastward equatorial jet develops peaking at about 1 m/s in autumn [Wyrki, 1973]. In the summer (JAS), a weak westward flow is observed in the west. Superimposed on this seasonal variability are interannual fluctuations closely linked to ENSO [see *e.g.* Cadet, 1985]. However, detailing these changes has been difficult in the absence of direct observations. Fortunately, extensive deployments of the 15m-drogued drifters were carried out as a part of the WOCE Global Data Surface Velocity Programme [Niiler *et al.*, 1987; Hansen and Poulain, 1996]. In this study we combine the drifter observations and the altimeter sea levels using a multivariate optimal interpolation algorithm to produce monthly mean surface currents in the Indian Ocean on a regular  $3^\circ \times 2^\circ$  grid. The resulting current analysis shows stunning changes in momentum and mass during the

1997-8 event and also reveals the coincidence of the Indian Ocean near-surface currents and the Pacific winds throughout the decade.

## 2. Data and analysis

This study is based on five data sets; altimeter sea level, 15m-drogued drifter velocity, climatological surface velocity estimates from historical shipdrift, Sea Surface Temperature (SST) data, and NCEP/NCAR reanalysis winds. The TOPEX/POSEIDON altimeter sea level is obtained from the Pathfinder version 2.1 archive [Koblinsky, personal communication, 1997]. This data spans the interval from late September 1992 through the end of our analysis period, October 2000, with a 9.92-day repeat cycle and a near-equatorial track spacing of  $2.8^\circ$ . After the usual corrections for geophysical effects, the sea level estimates have been averaged into  $1^\circ$  latitude segments.

Surface drifter currents are obtained from the WOCE/TOGA archive at the Atlantic Ocean Marine Laboratory (NOAA/AOML). The data spans the period February 1979 - October 2000. The drifter tracks are converted to six-hourly velocity estimates as described by Hansen and Poulain [1996]. These currents are averaged into  $2^\circ \times 3^\circ \times 1$ -month bins, which then form the basic data set for our study.

To provide a first guess for our analysis we also use ship-drift velocity estimates available on the Ocean Current Drifter Data CD-ROM provided by NOAA/NODC to construct a climatological monthly cycle of currents. The results of this preliminary analysis are very comparable with the climatology of Cutler and Swallow [1984], as described below. Our analysis includes ageostrophic effects estimated based on NCEP/NCAR reanalysis surface wind stress [Kalnay et al., 1996]. To evaluate the heat balance we use the SST provided by the analysis of Reynolds and Smith [1994]. Finally, we use independent 20-30m velocity estimates from shipboard Acoustic Doppler Current Profilers acquired from the Joint Archive for Shipboard ADCP at University of Hawaii to provide an independent estimate of velocity error.

The procedure for mapping surface currents follows the methodology of multivariate statistical interpolation [Daley, 1991; Grodsky and Carton, 2001]. Near surface velocity can be decomposed into a geostrophic component and winddrift. Following Lagerloef et al. [1999], we assume that the winddrift satisfies an Ekman-like equation balancing the difference between the wind-induced momentum flux and the linear friction with the Coriolis force. A simple linear friction term is included to allow an Ekman-like balance to account for the ageostrophic component on the equator. The geostrophic component of the mixed layer analysis velocity,  $\mathbf{u}^A$ , is then written as a linear combination of the weighted differences between the observations, ‘ $O$ ’, and the background estimates, ‘ $B$ ’, of sea level,  $\eta$ , and the mixed layer velocity,  $\mathbf{u}$ ,

$$\mathbf{u}^A = \mathbf{u}^B + \mathbf{W}^{\eta\eta}(\eta^O - \eta^B) + \mathbf{W}^{\mathbf{u}\mathbf{u}}(\mathbf{u}^O - \mathbf{u}^B) \quad (1)$$

The weights,  $\mathbf{W}$ , are determined by minimizing the least square expected error based on an estimate of the modeled error covariance, assumed here to be Gaussian with  $4.5^\circ$  and  $2.5^\circ$  zonal and meridional scales, respectively [following Carton et al., 2000]. We assume that the observations minus background differences are largely geostrophic and thus are able to use the geostrophic equations to relate pressure and velocity errors in (1). These

geostrophic error covariances are extended to the equatorial beta-plane based on the Kelvin Wave scaling of *Picaut et al.* [1989]. See also *Grodsky and Carton* [2001] for further details.

The background current estimates are constructed in two stages. First we use a combination of surface drifter and ship drift to compute time averaged currents. Using the time averaged currents as a preliminary background estimate, we combine altimeter sea level, drifter, and ship drift currents using (1) to construct a monthly climatology, part of which is presented in **Figure 1**, upper panel. In addition to being of interest by itself, this monthly climatology also serves as a nearly unbiased background estimate for our monthly analysis of near-surface velocity anomalies. An example of the anomaly analysis is presented in **Figure 1**, lower panel.

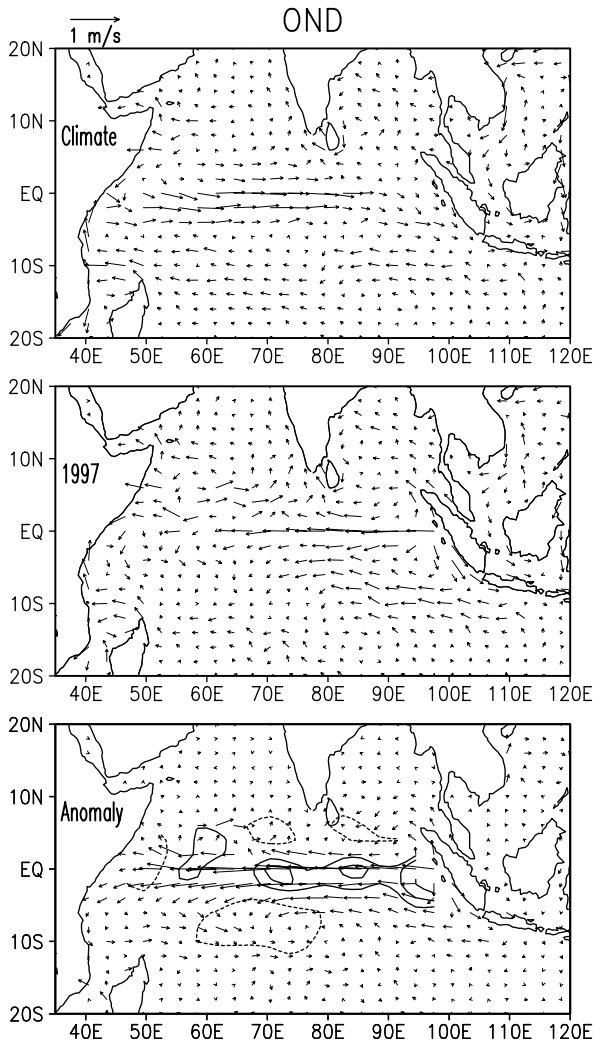


**Figure 1.** October-November-December average currents in the Indian Ocean: (top) climatology, (middle) year 1997, and (bottom) 1997 anomaly from climatological mean. Contours show anomalous current divergence at  $[-1, 1, 2, 4, 8] \cdot 10^{-7}$  1/s levels. Negative isolines are shown with dashed lines.

One way by which we can evaluate the accuracy of the velocity analysis is to compare our estimates to independent contemporaneous shipboard ADCP observations.

These observations are from 34 ship cruises primarily during the middle 1990s (the data of the 1999 Joint Air-Sea Monsoon Interaction Experiment, JASMINE, were not available for this comparison) but are widely distributed throughout the latitude range 20<sup>0</sup> S-20<sup>0</sup> N with better coverage in the north and east. The analysis currents at points where ADCP observations are available have a variance of 380 (m/s)<sup>2</sup>. The variance of deviation between analysis and ADCP currents is 150 (m/s)<sup>2</sup>, thus the velocity analysis explains 60% of the independent ADCP velocity variance. Since the ADCP measurements are essentially instantaneous, they contain a high, but difficult to evaluate, noise level when interpreted as monthly average estimates. Thus, a significant, but difficult to determine, part of the 40% unexplained variance may be due to interpretation error of the ADCP data.

### 3. Results

During the boreal fall the eastward Wyrтки jet and an eastward Indian Monsoon Current located slightly north of the equator develop in response to the summer monsoon winds [Wyrтки, 1973] (see **Figure 1**). South of the equator the South Equatorial Current (SEC) flows westward along 10<sup>0</sup> S in the eastern basin and shifts to 15<sup>0</sup> S west of 80<sup>0</sup> E. The contrast to conditions in 1997 is striking. During the fall of that year the surface currents on the equator became westward in response to a strengthening of the trade winds with anomalies exceeding 1 m/s and a significant meridional divergence. The SEC intensified also in the east while weakening in the west. The strongest equatorial divergence probably exists close to the coast of Sumatra where the anomalous flow is poleward on both sides of the equator and divergence exceeds 4\*10<sup>-7</sup> s<sup>-1</sup> (see **Figure 1**).

The development of the westward equatorial jet is clearly related to changes in the winds in the Indian Ocean sector. In the Pacific Ocean *Yu and McPhaden* [1999] found the near surface equatorial zonal momentum to be dominated by a three-term linear balance between local acceleration,  $\partial u / \partial t$ , zonal pressure gradient,  $-g\partial\eta / \partial x$ , and zonal wind stress,  $\tau^x$ , the first three terms of (2)

$$\frac{\partial u}{\partial t} = -g \frac{\partial \eta}{\partial x} + \frac{\tau^x}{\rho H} - au \quad (2)$$

Estimates of the vertical mixing lengthscale,  $H$ , vary. *Ralph and Niiler* [1999] summarize different approaches and have found that the estimate of  $H$  based on mixing length theory seems to fit the observations best, an approach which we generalize here to apply to frictional balances in near-equatorial regions, as  $H = u_*/(\gamma(f^2 + r^2)^{1/2} D^{1/4})$ . Here,  $f$  is the Coriolis parameter,  $u_*$  is the friction velocity in water, and  $\gamma = 0.17$  is fitting constant. The friction coefficient for winddrift currents,  $r$ , is chosen to be  $2.15*10^{-4}/D = 4.5*10^{-6} \text{ s}^{-1}$ , following *Lagerloef et al.* [1999], while  $D = 44$  m is an estimate of the mean mixed layer depth.

Here we consider the zonal momentum balance in the more narrow Indian Ocean expanded to include Rayleigh friction in (2). The terms along the equator, presented in **Figure 2**, show that the Indian Ocean is sufficiently narrow zonally that the annual period exceeds the equatorial adjustment time of the ocean and thus the anomalous wind-

induced momentum flux is almost completely balanced by the anomalous pressure gradient force throughout the 1990s. As a result, the anomalous zonal velocity varies almost in phase with wind forcing (**Figures 2c** and **2d**). **Figure 2d** shows the balance of Rayleigh friction with the remaining terms in (2) where  $a=(5\pm 3)*10^{-7} \text{ s}^{-1}$  is estimated from linear regression between the residual force and the anomalous zonal current. Substantial deviations in this balance do exist, mostly notably during 1997, but some of the deviations in this balance are the result of errors in the large pressure gradient and wind stress terms.

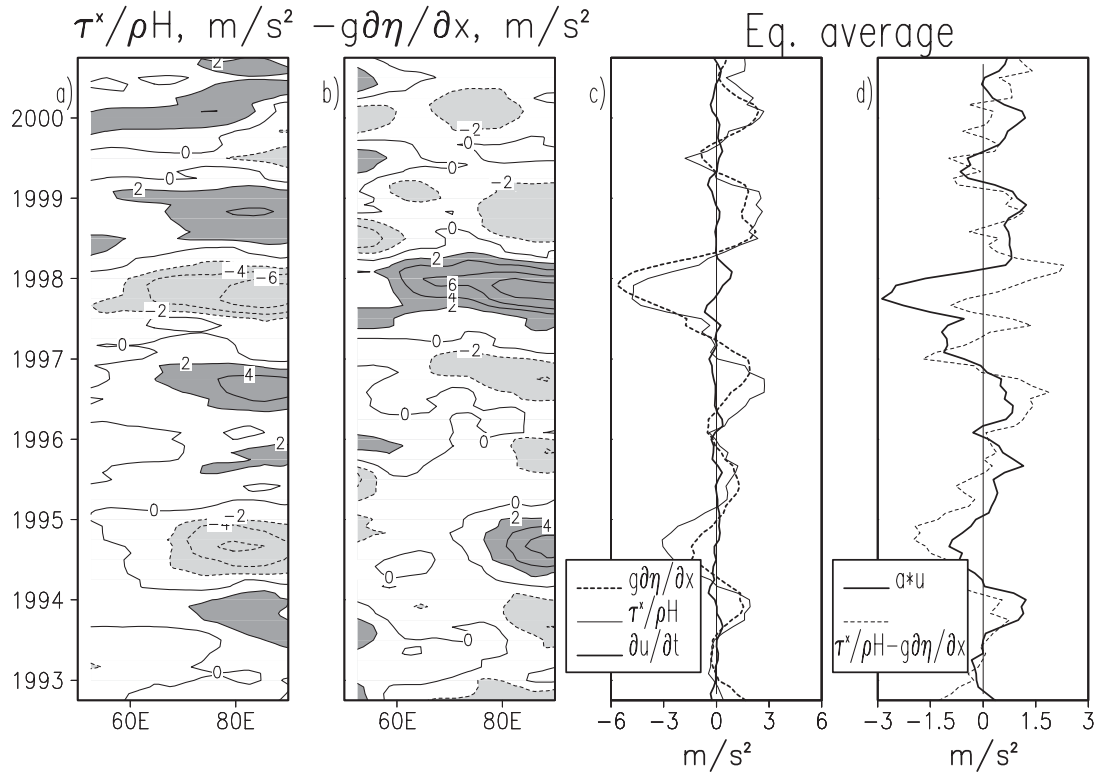


**Figure 2.** Time-longitude equatorial diagrams of (a) anomalous wind stress force and (b) pressure gradient force. Panel (c) shows zonal averages of the terms presented in (a, b) along with anomalous local acceleration. Panel (d) compares Rayleigh friction with the sum of the other terms. All values are multiplied by  $10^7$ .

The spatial structure of the ocean's response to interannual wind variability was explored by *Murtugudde et al.* [2000] who found through a series of numerical simulations that the dominant joint Empirical Orthogonal Function (EOF) of SST and winds describes a balanced response, including zonal dipole of SST along with an intensification of both trade wind systems in the east and northwesterly anomalies south of  $10^0 \text{ S}$ . Here we examine the spatial (longitude-latitude) structure of the response of the observed ocean in the same  $25^0 \text{ S}$ - $25^0 \text{ N}$ ,  $30^0 \text{ E}$ - $120^0 \text{ E}$  domain (**Figure 3**) for comparisons with their results. Although the EOFs of  $U$ ,  $\eta$ , and  $\tau$  are computed independently, the dominant components are reasonably well correlated in time ( $R^2 \sim 0.6$ ). The dominant EOF of the currents, explaining 50% of the variance (**Figure 3**), shows the main features of the equatorial currents discussed above including the 1 m/s strengthening of the westward Equatorial Jet in 1997 in response to intensifying easterly winds. South of  $4^0 \text{ S}$

the SEC intensifies in the east and attenuates in the west with a convergence in between. The sea level develops a strong westward gradient of  $\sim 0.5\text{cm/deg}$  along the equator with a 1-2 month time lag behind the winds reflecting the Kelvin/Rossby Wave adjustment time.

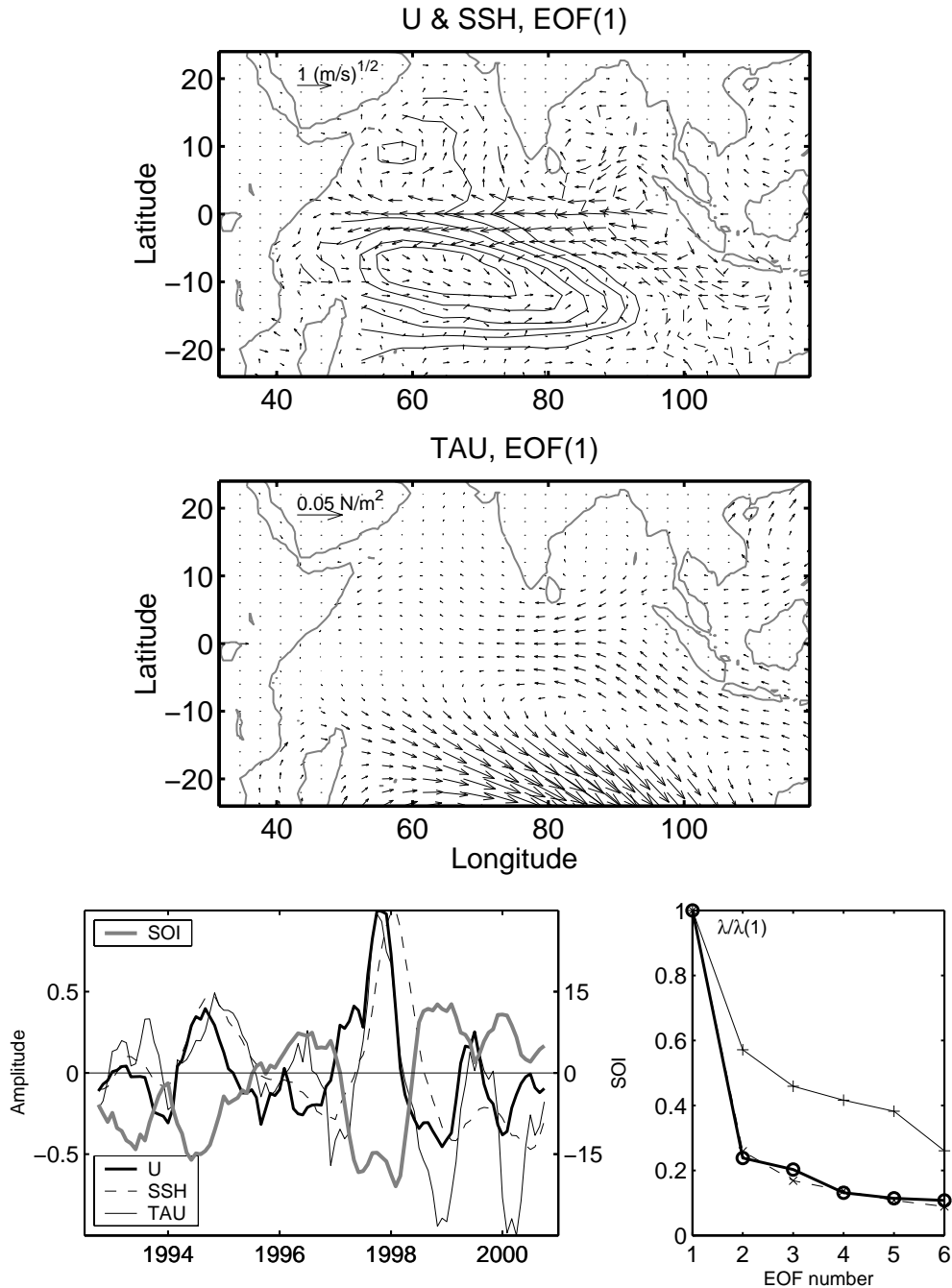


**Figure 3.** Leading interannual EOFs of surface velocity ( $\mathbf{u}$ ), sea level (SSH), and wind stress (TAU). The principal component time series along with the Southern Oscillation Index and relative sizes of eigenvalues are shown in the bottom line. Sea level contour of the vector field  $\mathbf{u}/(|\mathbf{u}|)^{1/2}$ .

In addition to transporting mass, the strong anomalies of near-surface currents may play an important role in heat transport. Uncertainties in both velocity and surface fluxes preclude the possibility of evaluating a monthly heat balance, as was done for momentum. However we can estimate the contribution of thermal advection to the 1997 dipole in SST by considering the more robust annual average budget. To evaluate this we use our velocity analysis to compute terms of the anomaly heat balance of the mixed layer calculated along the equator. Here water temperature is assumed homogeneous inside the mixed layer and equal to SST. The mixed layer depth,  $D$ , is provided by the *Carton et al.* [2000] ocean reanalysis. The results, presented in **Figure 4**, show that anomalous advection acting on the mean temperature gradient is, indeed, a dominant term in the balance that results in warming the west and cooling the east. In the eastern basin anomalous advection cools the ocean by westward transport of cold waters upwelled near the Java and Sumatra coasts. Conversely, the western basin is warmed by westward transport of the relatively warm waters of the central basin. The results show that anomalous advection is compensated for in part by surface heat flux. The sum of advective heat transport and net surface flux is close (to within  $\pm 10 \text{ W/m}^2$ ) to the local rate of change of the mixed layer heat content except near the eastern and western boundaries. Thus, the results presented here are generally consistent with the model simulations of *Murtugudde et al.* [2000] and make clear the key role of zonal advection acting on the mean temperature gradient in setting up the dipole pattern of SST so prominent in 1997-8.

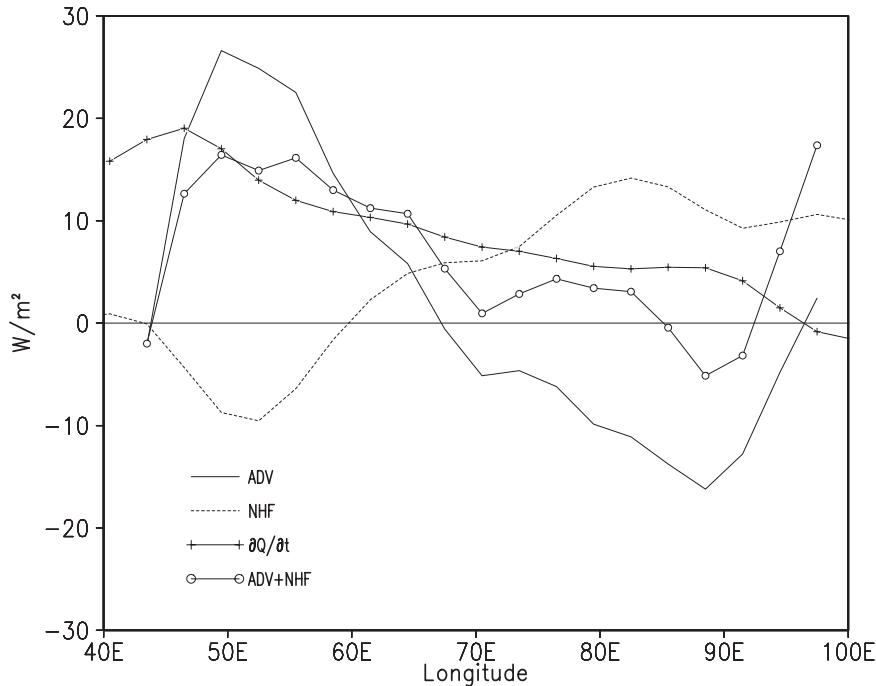


**Figure 4.** Terms in the anomalous heat budget along the equator, annually averaged for 1997. Terms include - rate of change of heat content,  $\partial Q / \partial t = C_p \rho (D \partial T / \partial t)$ , advection,  $ADV = -C_p \rho [D(u \partial T / \partial x + v \partial T / \partial y)]$ , net surface heat flux, NHF, based on NCEP/NCAR reanalysis surface heat fluxes. Also shown is the sum of advection and surface heat flux,  $ADV + NHF$ , which balances the time rate of change of heat content throughout much of the basin to within  $\pm 10 \text{ W/m}^2$ .

The 1993-2000 period covers two anomalous easterly wind events one during 1994 and the other during 1997. The 1994 event has been described by *Vinayachandaran et al.* [1999] who found a persistent easterly wind anomaly in the east (east of 70° E) beginning in April and lasting for at least 8 months. The 1997 event was stronger and observed well west of 60° E (see **Figure 2a**). As a result, the 1994 and 1997 events had quite similar cooling in the east, but there was no warming in the west in 1994 [*Murtugudde et al.*, 2000].

The strengthening of the easterly wind also prevents the development of the Wyrтки Jet, which appears during the transition periods between the monsoons. In contrast the fall transition period (OND) currents on the equator in 1997 were westward (see **Figure 1**). A similar but a weaker event took place in the second half of 1994. Our analysis for that year shows that the westward current anomaly was ~0.3 - 0.4 m/s, so that the Wyrтки jet developed but was weaker than the climatological one.

Both, the 1994 and 1997 events coincide in time with the ENSO events in the Pacific Ocean. Moreover, *Potemra and Lukas* [1999], *Susanto et al.* [2001], *Murtugudde* [private communication] as well as our analysis show that eastern equatorial Indian Ocean dynamics is intimately related to ENSO forcing at least during the decade of 1990s. Although longer time records demonstrate that a unique and inherent air-sea dynamics over the Indian Ocean contributes significantly [*Vinayachandaran et al.*, 1999].

## Acknowledgments

SG and JC gratefully acknowledge support from the National Science Foundation (OCE9812404) to JAC. RM would like to acknowledge NASA salinity and Indian Ocean grants. We are grateful to the Drifter DAC of the GOOS Center at NOAA/AOML for providing the drifter data set.

## References

- Cadet, D. L., The Southern oscillation over the Indian Ocean, *J. Climatol.*, **5**, 189-212, 1985.
- Carton, J. A., G. Chepurin, X. Cao, and B. Giese, A simple Ocean Data Assimilation analysis of the global upper ocean 1959-1995, Part 1: Methodology, *J. Phys. Oceanogr.*, **30**, 294-309, 2000.
- Cutler, A. N., and J. C. Swallow, Surface currents in the Indian Ocean (to 25S, 100E). *Rep. 187*, 42 pp., Inst. of Oceanogr. Sci., Wormley, England, 1984.
- Daley, R., Atmospheric Data Analysis, Cambridge University Press, 457 pp., 1991.
- Grodsky, S. A., and J. A. Carton. Intense surface currents in the Tropical Pacific during 1996-1998, *J. Geoph. Res.*, **106**, 16,673-16,684, 2001.
- Hansen, D. V., and P.-M. Poulain, Quality control and interpolations of WOCE-TOGA drifter data, *J. Atmos. Oceanic Technol.*, **13**, 900-909, 1996.
- Kalnay, E., and Coauthors, The NCEP/NCAR 40-year reanalysis project, *Bull. Amer. Meteor. Soc.*, **77**, 437-471, 1996.
- Lagerloef, G. S. E., G.T. Mitchum, R. B. Lukas, and P. P. Niiler, Tropical Pacific near surface currents estimated from altimeter, wind, and drifter data, *J. Geophys. Res.*, **104**, 23,313-23,326, 1999.
- Molinari, R. L., D. Olson, and G. Reverdin, Surface current distributions in the tropical Indian Ocean derived from compilations of surface buoy trajectories, *J. Geoph. Res.*, **95**, 7217-7238, 1990.
- Murtugudde, R., J. P. McCreary Jr., and A. J. Basalacchi, Oceanic processes associated with anomalous events in the Indian Ocean with relevance to 1997-1998, *J. Geophys. Res.*, **105**, 3295-3306, 1999.
- Niiler, P. P., R. E. Davis, and H. J. White, Water following characteristics of a mixed layer drifter, *Deep Sea Res., Part A*, **34**, 1867-1882, 1987.

- Picaut, J., S. P. Hayes, and M. J. McPhaden, Use of geostrophic approximation to estimate time-varying zonal currents at the equator, *J. Geophys. Res.*, **94**, 3228-3236, 1989.
- Potemra, J. T., and R. Lukas, Seasonal to interannual modes of sea level variability in the western Pacific and eastern Indian Oceans, *Geoph. Res. Lett.*, **26**, 365-368, 1999.
- Ralph, E. A., and P. P. Niiler, Wind-driven currents in the Tropical Pacific, *J. Phys. Oceanogr.*, **29**, 2121-2129, 1999.
- Rao, R. R., R. L. Molinary, and J. F. Fiesta, Evolution of the climatology near-surface thermal structure of the Indian Ocean. 1. Description of mean monthly mixed layer depth, and sea surface temperature, surface current, and surface meteorological fields, *J. Geophys. Res.*, **94**, 10,801-10,815, 1989.
- Reynolds, R. W., and T. M. Smith, Improved global sea surface temperature analyses using optimum interpolation, *J. Clim.*, **7**, 929-948, 1994.
- Saji, N. H., B. N. Goswami, P. N. Vinayachandran, and T. Yamagata, A dipole mode in the tropical Indian Ocean, *Nature*, **401**, 360-363, 1999.
- Susanto, R. D., A. L. Gordon, and Q. Zheng, Upwelling along the coast of Java and Sumatra and its relation to ENSO, *Geoph. Res. Lett.*, **28**, 8, 1599-1602, 2001.
- Webster, P. J., A. M. Moore, J. P. Loschnigg, and R. R. Leben, Coupled ocean-temperature dynamics in the Indian Ocean during 1997-98, *Nature*, **401**, 356-360, 1999.
- Yu, L. A., and M. M. Rienecker, Mechanisms for the Indian Ocean warming during the 1997-98 El Nino, *Geoph. Res. Lett.*, **26**, 735-738, 1999.
- Yu, X. R., and M. J. McPhaden, Dynamical analysis of seasonal and interannual variability in the equatorial Pacific, *J. Geophys. Res.*, **29**, 2350-2369, 1999.
- Vinayachandran, P.N., N.H. Saji, and T. Yamagata, Response of the Equatorial Indian Ocean to an unusual wind event during 1994, *Geoph. Res. Lett.*, **26**, 1613-1616, 1999.
- Wyrtki, K. Equatorial jet in Indian Ocean, *Science*, **181**, 264-266, 1973.